

Determination of standard Gibbs energies of formation of ternary oxides in the system Co-Sb-O by solid electrolyte emf method

K. SWAMINATHAN, O. M. SREEDHARAN

Thermodynamics & Kinetics Division, Indira Gandhi Centre for Atomic Research, Kalpakkam 603 102, India
E-mail: oms@igcar.ernet.in

An isothermal section of the phase diagram of the system Co-Sb-O at 873 K was established by isothermal equilibration and XRD analyses of quenched samples. The following galvanic cells were designed to measure the Gibbs energies of formation of the three ternary oxides namely CoSb_2O_4 , $\text{Co}_7\text{Sb}_2\text{O}_{12}$ and CoSb_2O_6 present in the system.

Chromel, Mo, Sb, CoO, CoSb_2O_4	15 CSZ	NiO, Ni, Mo, Chromel	I
Pt, CoO, $\text{Co}_7\text{Sb}_2\text{O}_{12}$, CoSb_2O_4	15 CSZ	air ($P_{\text{O}_2} = 0.21$ atm), Pt	II
Pt, $\text{Co}_7\text{Sb}_2\text{O}_{12}$, CoSb_2O_6 , CoSb_2O_4	15 CSZ	air ($P_{\text{O}_2} = 0.21$ atm), Pt	III

where 15 CSZ stands for ZrO_2 stabilized by 15 mol % CaO. The reversible emfs obtained could be represented by the following expressions.

$$E_I \pm 0.5 \text{ (mV)} = 120.7 - 0.04924 T(\text{K}) \quad (795\text{--}954 \text{ K})$$

$$E_{II} \pm 0.5 \text{ (mV)} = 1106.3 - 0.3992 T(\text{K}) \quad (790\text{--}1040 \text{ K})$$

$$E_{III} \pm 0.4 \text{ (mV)} = 967.9 - 0.4395 T(\text{K}) \quad (855\text{--}1035 \text{ K})$$

The standard Gibbs energies of formation of CoSb_2O_4 , $\text{Co}_7\text{Sb}_2\text{O}_{12}$ and CoSb_2O_6 were computed from the emf expressions:

$$\Delta G_f^\circ (\text{CoSb}_2\text{O}_4) \pm 4.3 \text{ (kJ mol}^{-1}\text{)} = -1006.3 + 0.3549 T(\text{K})$$

$$\Delta G_f^\circ (\text{Co}_7\text{Sb}_2\text{O}_{12}) \pm 10.5 \text{ (kJ mol}^{-1}\text{)} = -2834.5 + 0.9190 T(\text{K})$$

$$\Delta G_f^\circ (\text{CoSb}_2\text{O}_6) \pm 4.5 \text{ (kJ mol}^{-1}\text{)} = -1379.9 + 0.5115 T(\text{K})$$

The reasonability of the above data were assessed by computing the entropy change for the solid-solid reactions leading to the formation of ternary oxides from the respective pairs of constituent binary oxides. © 2001 Kluwer Academic Publishers

1. Introduction

The thermodynamic stabilities of inter-oxide compounds in the systems M-Sb-O (where M = Fe, Cr or Ni) are of relevance in evaluating the Fission Product-Clad Chemical Interaction (FPCCI) in Fast Breeder Reactors (FBRs) since antimony is one of the deleterious fission products though minor in yield [1]. In addition, Sb_2O_3 (in the valentinite form) encapsulated in stainless steel was found to pose compatibility problem when used in the neutron source which is an in-core component in some FBRs [2]. Hence, a systematic investigation of the stabilities of ternary oxides in the systems Cr-Sb-O and Ni-Sb-O were carried out by Swaminathan and Sreedharan by employing the familiar solid oxide electrolyte emf technique [3, 4]. Though cobalt is neither a constituent of the structural alloy of

FBRs nor a fission product still the stabilities of inter-oxide compounds in the system Co-Sb-O would be of considerable interest in understanding the systematic trend if any among the isomorphous analogs of triad elements Fe, Co and Ni. To facilitate an investigation of the stabilities of ternary compounds CoSb_2O_4 , $\text{Co}_7\text{Sb}_2\text{O}_{12}$ and CoSb_2O_6 present in the system Co-Sb-O, no reliable phase diagram has so far been reported in the literature. However, three intermetallic phases CoSb, CoSb_2 and CoSb_3 and four binary oxides CoO, Co_3O_4 , Sb_2O_3 and Sb_2O_4 are known to be stable in the temperature range of 800–1100 K [5]. On the basis of these information a systematic study of the phase diagram of the system Co-Sb-O as well as the thermodynamic stabilities of the ternary oxides in this system were undertaken.

The present study may also be of relevance to materials science and technology owing to the use of CoSb_2O_6 as an oxidation catalyst [6], metal oxide resistor material [7] as well as in ion exchange [8]. Besides CoSb_2O_6 , $\text{Co}_7\text{Sb}_2\text{O}_{12}$ finds application in ZnO varistors [9]. Incidentally, CoSb_2O_6 crystallizes in a trirutile type structure with space group $\text{P4}_2/\text{mmm}$ [10] while $\text{Co}_7\text{Sb}_2\text{O}_{12}$ exists as a spinel (space group $\text{Fd } 3\text{m}$) [11] and CoSb_2O_4 exhibits Pb_3O_4 structure which is isomorphous with NiSb_2O_4 with space group $\text{P4}_2/\text{mbc}$ [12].

2. Experimental

2.1. Materials

Co (Robert Johnson), Co_3O_4 (Aldrich), Sb and Sb_2O_3 (Johnson Matthey) of purity better than 99.99% were used as starting materials. Sb_2O_4 was prepared by oxidation of Sb_2O_3 in air at 823 K with intermittent grinding of the product to ensure completion of oxidation. CoO was prepared by heating Co_3O_4 at 1273 K under a dynamic vacuum of 1 mPa. CoSb_2O_6 was synthesised by compacting an equimolar mixture of CoO and Sb_2O_4 into cylindrical pellets of 10 mm diameter and 5 mm thickness in a hydraulic press at a pressure of 100 MPa. These pellets were heated in ambient air at 873 K and 1173 K for a total period of 96 h. This process was repeated at least twice to complete the reaction. Formation of ternary oxide was verified by powder X-ray Diffraction (XRD) technique within a 5 mass % limit of its detection of impurity phases. A 6 : 1 mixture of CoO and CoSb_2O_6 was likewise compacted after thorough mixing for the preparation of $\text{Co}_7\text{Sb}_2\text{O}_{12}$. The pellets were encapsulated in evacuated silica ampoules after outgassing at 473 K and was subsequently heat treated at 873 K for a prolonged period of 600 h. A similar heat treatment was given to pellets made from 1 : 1 mixture of CoO and Sb_2O_3 for the synthesis of CoSb_2O_4 . A 15 mol % (15 CSZ) calcia-stabilised zirconia tube (Yamari, Japan) with one end closed and closed end flat of dimensions 12.5 mm OD, 9.5 mm ID and 305 mm long with density better than 98% of the theoretical value, was used as the solid electrolyte in two com-

partment cell assembly for the galvanic cell configurations employing air/Pt as reference electrode. The same material in the form of cylindrical discs of diameter 12.5 mm and 1.5 mm thickness (Yamari, Japan) was used as the solid electrolyte in the other cell with solid electrodes arranged in a stacked pellet configuration.

2.2. Procedure

2.2.1. Phase equilibrium studies

Mixtures of various phases as given in Table I were made by grinding the component phases in an agate mortar. The resulting mixtures were compacted into pellets as described earlier. Those mixtures which require vacuum heat treatment were encapsulated in silica ampoules. The ampoules were outgassed at temperatures up to 473 K prior to sealing under vacuum. Powder mixtures stable in air were heat treated in the ambient atmosphere. All the heat treatments were carried out at an isothermal temperature of 873 K for a total period of 600 h, with at least one intermediate grinding and recompaction, followed by air quenching. The phase identification was accomplished using XRD.

2.2.2. Emf studies

The following galvanic cells,

Chromel, Mo, Sb, CoO, CoSb_2O_4	15 CSZ	NiO, Ni, Mo, Chromel	I
Pt, CoO, $\text{Co}_7\text{Sb}_2\text{O}_{12}$, CoSb_2O_4	15 CSZ	air ($P_{\text{O}_2} = 0.21 \text{ atm}$), Pt	II
Pt, $\text{Co}_7\text{Sb}_2\text{O}_{12}$, CoSb_2O_6 , CoSb_2O_4	15 CSZ	air ($P_{\text{O}_2} = 0.21 \text{ atm}$), Pt	III

were studied over the temperature ranges 795–954 K, 790–1040 K and 855–1035 K respectively.

An open cell stacked pellet assembly described elsewhere [13] was used for measurements on cell I. In order to prevent the attack of electrical lead wires and contact foils by antimony, a molybdenum foil of 12 mm

TABLE I Results of phase equilibrium studies of the Co-Sb-O system at 873 K

S. no.	Before equilibration		Condition of equilibration	After equilibration phases found
	Phases	Co : Sb : O		
1.	Co_3O_4 , Sb_2O_4	3 : 3 : 10	air	Co_3O_4 , CoSb_2O_6
2.	Co_3O_4 , Sb_2O_4	3 : 8 : 20	air	CoSb_2O_6 , Sb_2O_4
3.	Co_3O_4 , Sb_2O_4	3 : 6 : 10	air	CoSb_2O_6
4.	Co_3O_4 , Sb_2O_4	6 : 3 : 14	vacuum*	Co_3O_4 , CoSb_2O_6 , $\text{Co}_7\text{Sb}_2\text{O}_{12}$
5.	CoO, Sb_2O_4	9 : 4 : 17	vacuum*	CoO, $\text{Co}_7\text{Sb}_2\text{O}_{12}$, CoSb_2O_4
6.	Co_3O_4 , Sb_2O_4 , Sb_2O_3	9 : 6 : 22	vacuum*	CoSb_2O_4 , CoSb_2O_6 , $\text{Co}_7\text{Sb}_2\text{O}_{12}$
7.	CoO, Sb_2O_3	2 : 2 : 5	vacuum*	CoO, CoSb_2O_4
8.	CoO, Sb_2O_3	1 : 4 : 7	vacuum*	CoSb_2O_4 , Sb_2O_3
9.	CoO, Sb_2O_3	1 : 2 : 4	vacuum*	CoSb_2O_4
10.	Co_3O_4 , Sb_2O_4	3 : 10 : 24	vacuum*	CoSb_2O_6 , Sb_2O_3
11.	CoO, Sb_2O_3 , Sb	1 : 3 : 4	vacuum*	CoSb_2O_4 , Sb
12.	CoO, Sb_2O_3	3 : 2 : 6	vacuum*	CoO, Sb
13.	CoO, Co, Sb	2 : 4 : 1	vacuum*	CoO, CoSb_3 , Sb
14.	CoO, Co, Sb	3 : 5 : 1	vacuum*	CoO, CoSb_2 , CoSb_3
15.	CoO, Co, Sb	3 : 3 : 1	vacuum*	CoO, CoSb , CoSb_2
16.	CoO, Co, Sb	3 : 1 : 1	vacuum*	CoO, CoSb , Co

*static vacuum in sealed silica ampoules.

diameter and 0.1 mm thickness was employed as spacer between the identical chromel leads and the electrode pellets. For the galvanic cells II and III, a two compartment cell assembly with 15 CSZ tube separating the two electrode compartments was employed, the details of which are described elsewhere [14–17]. Helium gas of spectroscopic purity, dried by passage through columns of silica gel and outgassed molecular sieve (Linde 4A), was used as the common inert gas in cell I and for protecting the test electrode in cells II and III. The cells were located in the isothermal zone of a bifilar wound furnace with an earthed shield to ground the induced electrical noise. The absence of spurious contribution to cell emf was confirmed by nearly null emf values (± 0.5 mV) obtained with a symmetrical cell employing identical Ni/NiO pellet electrodes in cell I together with Mo spacers and chromel lead wires in the temperature range 700–1200 K. Similar null emf (within ± 1 mV) was obtained over the same temperature range with a symmetric cell in the two compartment configuration when both platinum electrodes were exposed to ambient air. The temperature measurements were made by a type S thermocouple duly calibrated at the freezing points of Sn, Zn, Sb and Ag. The performance of cell I was checked using Ni + NiO and Cu + Cu₂O as electrodes. The emf was close to derived values computed from the standard Gibbs energies of formation of NiO and Cu₂O assessed by Kellog [18]. In the case of two compartment cell assembly, the emf of the cell, Pt, air ($P_{O_2} = 0.21$ atm) || O₂ (1 atm), Pt was also tested over the above temperature range and was found to deviate by less than 1 mV from the derived value calculated using the Nernst equation.

The test electrode for cell I was made from a mixture of CoO|CoSb₂O₄|Sb in the weight ratio 2 : 2 : 1 and the reference electrode, Ni|NiO was taken in the weight ratio 5 : 1. These mixtures were separately ground and compacted into discs of 10 mm diameter and 1–2 mm thickness as mentioned above. For cell II, a mixture of CoO|Co₇Sb₂O₁₂|CoSb₂O₄ and for cell III Co₇Sb₂O₁₂|CoSb₂O₆|CoSb₂O₄ in an equal weight ratio were ground and similarly compacted. These electrode compositions were nominal. A 10% variation in the weight ratio of all the three test electrodes was made in order to ascertain the existence of composition independent emf values. This procedure ensured that these three phases were truly in equilibrium with each other. The emfs obtained with different ratios of phases at the electrode are identified by separate designations such as A, B & C in Tables II–IV. Titanium sponge pieces in suitable location away from the cell leads were used as ‘*in situ*’ oxygen getters in both the cell configurations. The reproducibility of the emf values were tested by thermal cycling and micropolarisation.

3. Results and discussion

3.1. Phase equilibrium studies

The results of phase equilibrium studies are summarised in Table I. The column one of this table lists the compounds/elements taken, together with the composition expressed in atom ratios. Phase analyses after the heat treatment in either air or vacuum are also given in Table I. The average composition of the samples are

TABLE II Emf of cell I

S. no.	T(K)	E(mV)
Cell A		
1	879.5	76.9
2	868.5	77.5
3	889.5	76.0
4	901.0	75.9
5	815.0	80.4
6	837.0	80.2
7	858.0	78.8
8	880.0	77.2
9	901.0	75.7
10	828.0	80.3
11	848.0	78.7
12	869.0	77.4
13	892.0	76.8
14	912.0	76.5
15	923.0	75.9
16	933.0	75.3
Cell B		
17	816.0	80.1
18	846.0	79.4
19	879.5	77.7
20	912.5	76.4
21	932.0	75.7
22	954.0	74.6
Cell C		
23	866.0	77.7
24	877.0	77.5
25	856.5	78.5
26	835.5	79.9
27	856.5	79.1
28	878.0	77.9
29	866.5	78.1
30	845.0	79.5
31	824.0	80.4
32	835.5	80.0
33	857.0	78.4
34	878.5	77.5
35	898.5	75.6
36	889.5	76.2
37	846.0	78.8
38	856.5	78.5
39	869.0	77.8
40	878.5	77.1
41	890.0	76.4
42	900.5	75.9
Cell D		
43	795.0	81.8
44	815.0	81.2
45	836.0	79.7
46	858.0	79.2
47	879.5	77.4
48	901.0	76.1
49	825.5	80.0
50	847.5	78.5
51	868.0	77.2
52	888.5	76.1
53	909.5	75.6
54	930.0	75.1

shown by filled circles in Fig. 1. By combining information on the average composition with the phase analyses of equilibrated samples tie-lines were constructed. The equilibrium diagram thus established shows three 3-phase regions which are useful to the present study.

These three phase fields, namely CoO/CoSb₂O₄/Sb, CoO/Co₇Sb₂O₁₂/CoSb₂O₄ and Co₇Sb₂O₁₂/CoSb₂O₆/CoSb₂O₄ establish an unique oxygen potential at constant temperature. The oxygen potential can be measured by solid state cells based on stabilized-zirconia

TABLE III Emf of cell II

S. no.	T(K)	E(mV)
Cell A		
1	807.0	784.0
2	823.5	777.6
3	790.0	791.0
4	823.0	778.4
5	840.0	770.0
6	857.0	764.0
7	873.5	757.8
8	873.0	758.1
9	888.0	751.8
10	904.0	744.8
11	921.0	739.0
12	913.0	741.4
13	929.0	736.0
14	936.5	733.1
15	944.0	730.0
16	952.0	727.0
17	960.0	723.3
18	967.5	719.7
19	976.5	716.0
20	983.5	713.1
21	991.5	710.1
22	1010.0	703.1
23	1016.0	700.2
24	1024.0	697.1
25	1031.0	694.8
26	921.0	738.0
27	880.0	754.1
28	928.0	735.5
29	975.5	716.5
30	1024.0	697.3
Cell B		
31	896.0	748.9
32	911.0	742.6
33	928.0	736.0
34	943.0	730.0
35	958.5	724.2
36	975.5	717.0
37	990.0	711.4
38	981.5	715.0
39	965.5	721.6
40	951.0	726.8
41	936.0	732.2
42	919.0	739.0
43	903.0	746.3
44	887.5	752.5
45	872.0	758.0
46	919.0	739.0
47	847.5	767.8
48	896.5	748.9
49	943.5	729.6
50	990.0	711.3
51	1039.5	691.4

as the electrolyte. Incidentally the intermetallics CoSb and CoSb₂ are reported to exhibit compositional range of 48–51% and 64–67% of Sb respectively [5]. These intermetallics were found to coexist with CoO. In the absence of quantitative estimates of oxygen solubility limits in these intermetallics, these phases are represented only as points in the Co-Sb axis and tie-lines joining CoO are therefore shown as simple lines instead of as areas.

3.2. Emf measurements

The emf results on cells I, II and III are listed in Tables II–IV and are plotted in Figs. 2–4 respectively

TABLE IV Emf of cell III

S. no.	T(K)	E(mV)
Cell A		
1	904.0	570.8
2	920.0	563.6
3	935.0	557.3
4	951.0	550.5
5	966.0	543.2
6	951.0	549.5
7	920.0	563.2
8	905.0	570.5
9	967.0	542.3
10	983.0	536.3
11	904.5	570.5
12	921.5	562.8
13	937.5	556.0
14	953.0	548.6
Cell B		
15	938.0	555.7
16	953.0	548.9
17	970.0	542.4
18	985.0	534.7
19	1001.5	528.1
20	970.0	541.5
21	929.0	559.6
22	944.0	553.1
23	960.0	545.6
24	976.5	538.9
25	991.5	532.1
26	1005.0	526.2
27	1020.0	519.4
28	1035.0	512.9
Cell C		
29	855.0	591.5
30	871.0	584.9
31	887.5	577.0
32	888.5	576.9
33	904.0	571.5
34	919.5	564.7
35	936.0	557.5
36	896.5	574.5
37	913.0	567.6
38	929.0	559.2
39	863.5	587.9
40	888.0	577.1
41	920.0	564.3
42	952.0	549.1
43	983.5	535.4
44	1010.5	523.3

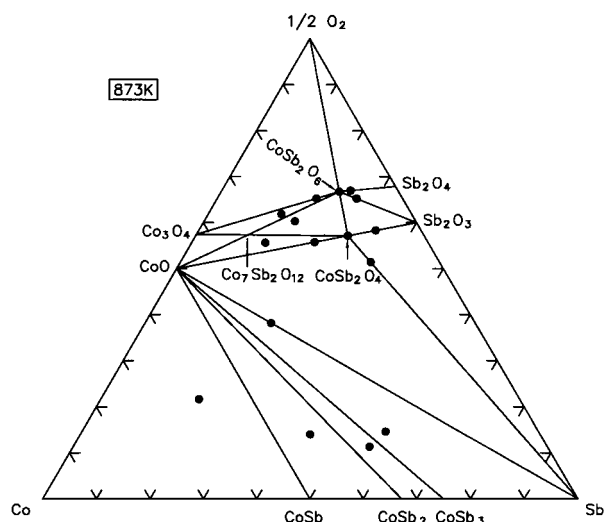


Figure 1 Isothermal section of the phase diagram for the system Co-Sb-O at 873 K.

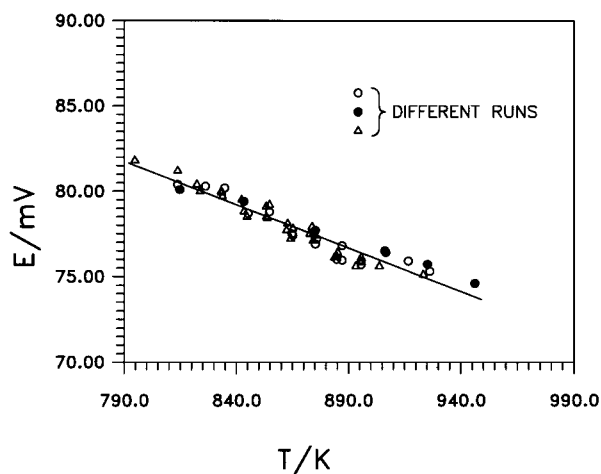


Figure 2 Variation of the reversible emf of cell I with temperature.

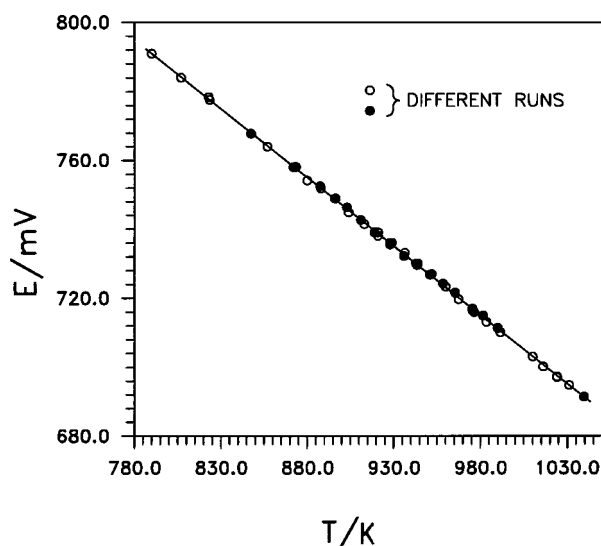


Figure 3 Temperature dependence of the reversible emf of cell II.

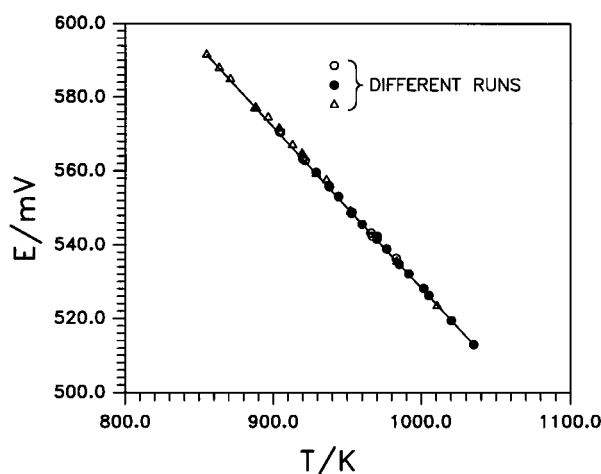


Figure 4 Temperature dependence of the reversible emf of cell III.

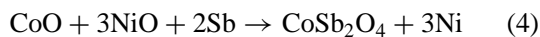
as a function of temperature. The emf appears to vary linearly with temperature. The least-square regression analyses give the following expressions valid over the respective temperature ranges listed in parenthesis.

$$E_{\text{I}} \pm 0.5 \text{ (mV)} = 120.7 - 0.0492 T \text{ (K)} \quad (795\text{--}954 \text{ K}) \quad (1)$$

$$E_{\text{II}} \pm 0.5 \text{ (mV)} = 1106.3 - 0.3992 T \text{ (K)} \quad (790\text{--}1040 \text{ K}) \quad (2)$$

$$E_{\text{III}} \pm 0.4 \text{ (mV)} = 967.9 - 0.4395 T \text{ (K)} \quad (855\text{--}1035 \text{ K}) \quad (3)$$

The overall virtual reaction corresponding to 6F of electricity for the galvanic cell I is



The standard Gibbs energy change corresponding to reaction (4) is calculated from the emf using the Nernst equation, ($\Delta G_{\text{R}}^{\circ} = -6FE$)

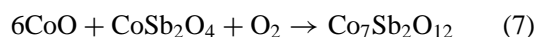
$$\Delta G_{\text{R}(4)}^{\circ} \pm 0.3 \text{ (kJ mol}^{-1}\text{)} = -69.9 + 0.0285 T \text{ (K)} \quad (5)$$

By combining Equation 5 with the literature data for $\Delta G_{\text{f}}^{\circ}$ of NiO and CoO [18,15], the standard Gibbs energy of formation, $\Delta G_{\text{f}}^{\circ}$ (CoSb₂O₄) could be calculated and is given below

$$\begin{aligned} \Delta G_{\text{f}}^{\circ} (\text{CoSb}_2\text{O}_4) \pm 4.3 \text{ (kJ mol}^{-1}\text{)} \\ = -1006.3 + 0.3549 T \text{ (K)} \end{aligned} \quad (6)$$

The uncertainty limit in $\Delta G_{\text{f}}^{\circ}$ (CoSb₂O₄) is obtained by combining the uncertainty limit of ± 3 kJ estimated for 3 moles of NiO from its $\Delta G_{\text{f}}^{\circ}$ (NiO) value assessed by Kellogg [18] and uncertainty limit of ± 1 kJ for CoO [19] with the uncertainty limit in Equation 5. The temperature dependent term in the above expression (6) which is related to the entropy of formation of the compound appears to be quite reasonable as it is comparable with twice the value of the relative partial molar entropy of oxygen.

The overall virtual reaction corresponding to 4F of electricity for the galvanic cell II is,



The standard Gibbs energy change corresponding to reaction (7) was calculated from the emf expression (2) after correcting for standard state of oxygen in the reference air/Pt electrode of cell II using Nernst equation

$$\Delta G_{\text{R}(7)}^{\circ} \pm 0.2 \text{ (kJ mol}^{-1}\text{)} = -427.0 + 0.1411 T \text{ (K)} \quad (8)$$

By combining Equation 8 with the literature data on CoO [15] and $\Delta G_{\text{f}}^{\circ}$ (CoSb₂O₄) derived above, the $\Delta G_{\text{f}}^{\circ}$ (Co₇Sb₂O₁₂) could be calculated and is given below:

$$\begin{aligned} \Delta G_{\text{f}}^{\circ} (\text{Co}_7\text{Sb}_2\text{O}_{12}) \pm 10.5 \text{ (kJ mol}^{-1}\text{)} \\ = -2834.5 + 0.9190 T \text{ (K)} \end{aligned} \quad (9)$$

The uncertainty limit in $\Delta G_{\text{f}}^{\circ}$ (Co₇Sb₂O₁₂) is obtained by combining the uncertainty limit in Equations 6 and 8 with an uncertainty limit of 6 kJ estimated for 6 moles of CoO [19]. The temperature dependent term in the above expression (9) which is related to the entropy of formation of the compound appears to be quite reasonable as it compares well with six times the value of the relative partial molar entropy of oxygen.

The overall virtual reaction for the galvanic cell III corresponding to 4F of electricity could be given as



The third phase $\text{Co}_7\text{Sb}_2\text{O}_{12}$ being an inert component was included mainly to unequivocally fix the oxygen potential by phase rule consideration. The $\Delta G_{\text{R}}^{\circ}$ for the Equation 10 was calculated by combining expression (3) with Nernst equation after correcting for standard state of oxygen in the reference air/Pt electrode of cell III and is given by

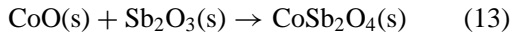
$$\Delta G_{\text{R}(10)}^{\circ} \pm 0.2 (\text{kJ mol}^{-1}) = -373.6 + 0.1566 T (\text{K}) \quad (11)$$

By combining the Equations 6 and 11, an expression for $\Delta G_{\text{f}}^{\circ}$ (CoSb_2O_6) was obtained and is given as

$$\begin{aligned} \Delta G_{\text{f}}^{\circ} (\text{CoSb}_2\text{O}_6) \pm 4.5 (\text{kJ mol}^{-1}) \\ = -1379.9 + 0.5115 T (\text{K}) \end{aligned} \quad (12)$$

The uncertainty limit in $\Delta G_{\text{f}}^{\circ}$ is obtained by combining those for Equations 6 and 11.

The expressions (6), (9) and (12) for the $\Delta G_{\text{f}}^{\circ}$ of the inter-oxide compounds included the uncertainties in the $\Delta G_{\text{f}}^{\circ}$ of the constituent binary oxides. However, the standard Gibbs energies of formation, $\Delta G_{\text{f,ox}}^{\circ}$ of the ternary oxides from the constituent binary oxides would be of greater relevance from the solid state chemistry point of view. The $\Delta G_{\text{f,ox}}^{\circ}$ (CoSb_2O_4) corresponding to the reaction



was calculated by combining $\Delta G_{\text{R}}^{\circ}$ for the cell I with $\Delta G_{\text{f}}^{\circ}$ of NiO [18] and Sb_2O_3 [20].

$$\begin{aligned} \Delta G_{\text{f,ox}}^{\circ} (\text{CoSb}_2\text{O}_4) = \Delta G_{\text{R}(4)}^{\circ} - \Delta G_{\text{f}}^{\circ} (\text{Sb}_2\text{O}_3, \text{s}) \\ + 3\Delta G_{\text{f}}^{\circ} (\text{NiO}) \end{aligned} \quad (14)$$

For computing $\Delta G_{\text{f,ox}}^{\circ}$ of $\text{Co}_7\text{Sb}_2\text{O}_{12}$ the reaction considered was



The Gibbs energy change, $\Delta G_{\text{f,ox}}^{\circ}$ ($\text{Co}_7\text{Sb}_2\text{O}_{12}$) corresponding to the above reaction was computed from the following expressions by an appropriate combination of $\Delta G_{\text{R}(7)}^{\circ}$ with $\Delta G_{\text{f}}^{\circ}$ of necessary binary oxides.

$$\begin{aligned} \Delta G_{\text{f,ox}}^{\circ} (\text{Co}_7\text{Sb}_2\text{O}_{12}) = \Delta G_{\text{R}(7)}^{\circ} - \Delta G_{\text{f}}^{\circ} (\text{Sb}_2\text{O}_5) \\ - \Delta G_{\text{f}}^{\circ} (\text{CoO}) + \Delta G_{\text{f}}^{\circ} (\text{CoSb}_2\text{O}_4) \end{aligned} \quad (16)$$

Likewise, $\Delta G_{\text{f,ox}}^{\circ}$ (CoSb_2O_6) was calculated from $\Delta G_{\text{R}(10)}^{\circ}$ by employing the expression

$$\begin{aligned} \Delta G_{\text{f,ox}}^{\circ} (\text{CoSb}_2\text{O}_6) = \Delta G_{\text{R}(10)}^{\circ} - \Delta G_{\text{f}}^{\circ} (\text{CoO}) \\ - \Delta G_{\text{f}}^{\circ} (\text{Sb}_2\text{O}_5) + \Delta G_{\text{f}}^{\circ} (\text{CoSb}_2\text{O}_4) \end{aligned} \quad (17)$$

for the following reaction



TABLE V $\Delta G_{\text{f,ox}}^{\circ}$ of inter-oxide compounds in the system Co-Sb-O

Compound	$\Delta G_{\text{f,ox}}^{\circ}$ (kJ mol ⁻¹) = $A + B T$ (K)	Standard deviation kJ mol ⁻¹
CoSb_2O_4	$-86.4 + 0.0385 T$	± 4.1
$\text{Co}_7\text{Sb}_2\text{O}_{12}$	$-205.5 - 0.0547 T$	± 5.8
CoSb_2O_6	$-152.1 - 0.0391 T$	± 5.8

For computing the numerical expressions for the above Equations one requires $\Delta G_{\text{f}}^{\circ}$ of Sb_2O_5 which is unstable in the temperature range of our consideration and is reported to dissociate into Sb_2O_4 and O_2 at 798 K in air. However, for the computation of $\Delta G_{\text{f,ox}}^{\circ}$ of inter-oxide compounds the following expression

$$\Delta G_{\text{f}}^{\circ} (\text{Sb}_2\text{O}_5) \pm 9.0 (\text{kJ mol}^{-1}) = -994.2 + 0.4802 T (\text{K}) \quad (19)$$

which is computed from the Gibbs energy data for Sb_2O_5 tabulated up to 798 K in the literature [21] is made use of. In making use of this expression its validity over a range extrapolated up to the temperature of the present measurement was assumed. These results are listed in Table V. The entropy change for the solid-solid reactions (13), (15) and (18) are not objectionably large as seen from the expressions listed in Table V and hence can be considered as reasonable.

No reliable calorimetric data are available to facilitate calculation of the standard enthalpies of formation, $\Delta H_{\text{f,298}}^{\circ}$ for these ternary oxides. Hence, values of -1006 ± 15 , -2835 ± 20 and -1380 ± 15 kJ mol⁻¹ could be taken as reasonable estimates of standard enthalpies of formation, $\Delta H_{\text{f,298}}^{\circ}$ of the inter-oxide compounds CoSb_2O_4 , $\text{Co}_7\text{Sb}_2\text{O}_{12}$ and CoSb_2O_6 respectively by second law.

The consistency of the Gibbs energy data on the inter-oxides determined from emf measurements with the phase diagram studies reported here was assessed as follows. For instance, in the region defined by the phases CoSb_2O_6 , Sb_2O_4 , Sb_2O_3 and CoSb_2O_4 at the four vertices of a quadrilateral in Fig. 1, two diagonal tie-lines are possible namely the one linking CoSb_2O_6 with Sb_2O_3 and CoSb_2O_4 with Sb_2O_4 . By making use of the $\Delta G_{\text{f}}^{\circ}$ of the ternary phases from the expressions (6) and (12) and those for binary oxides from literature [20, 22], the $\Delta G_{\text{R}}^{\circ}$ for the balanced reaction



was computed and at 873 K it was found to yield a value of -57.7 kJ. This upholds the fact that the pair of phases on the right hand side would form the tie-line. This inference is consistent with the experimental phase equilibrium studies (as shown in Fig. 1). A similar check was conducted for the region defined by the phases $\text{Co}_7\text{Sb}_2\text{O}_{12}$, CoSb_2O_6 , Sb_2O_3 and CoSb_2O_4 in Fig. 1, by making use of the balanced reaction



This yielded a value of -250 kJ at 873 K for the Equation 21, confirming the tie-line between CoSb_2O_6

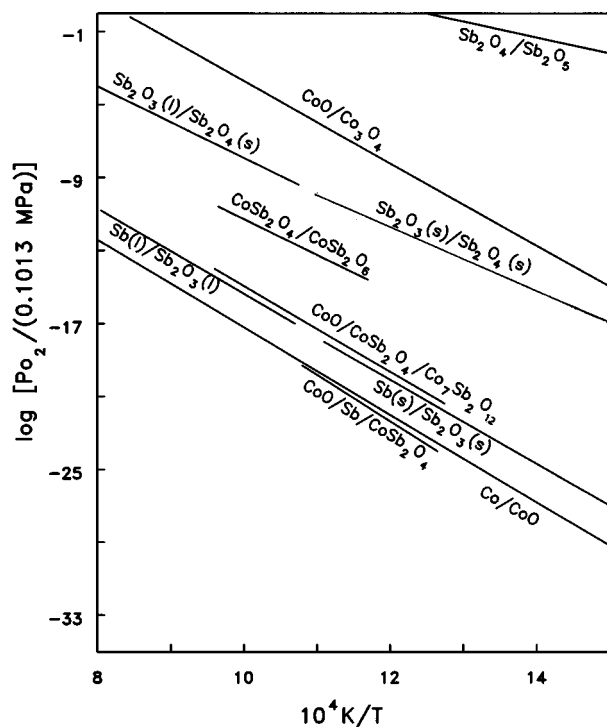


Figure 5 Variation of the logarithm of oxygen partial pressure with reciprocal of absolute temperature for condensed phase mixtures in the system Co-Sb-O.

and CoSb_2O_4 in agreement with experimental phase analysis.

After establishing the reliability of Gibbs energy data it would be worthwhile to compare the relative stabilities of the different oxygen buffer mixtures of phases with a $\log P_{\text{O}_2}$ - reciprocal absolute temperature diagram as shown in Fig. 5. This diagram shows not only the buffer mixtures employed in the emf studies on the three cells I, II and III but also the plots corresponding to the constituent binary oxides. There is no intersection of lines, signalling that the phase equilibria are invariant with temperature within the temperature range of measurements.

4. Conclusion

An isothermal section of the phase diagram for the system Co-Sb-O at 873 K was established in the study reported here. The standard Gibbs energies of formation of the three inter-oxide compounds are also reported here for the first time. The data were essentially derived from oxygen potential measurements from solid oxide electrolyte galvanic cells I, II and III whose equilibrium oxygen pressures could be represented by the following expressions.

$$\log [P_{\text{O}_2}/(0.1013 \text{ MPa})]_{\text{I}} = 9.90 - 26908/T(\text{K}) \quad (22)$$

$$\log [P_{\text{O}_2}/(0.1013 \text{ MPa})]_{\text{II}} = 7.37 - 22301/T(\text{K}) \quad (23)$$

$$\log [P_{\text{O}_2}/(0.1013 \text{ MPa})]_{\text{III}} = 8.18 - 19511/T(\text{K}) \quad (24)$$

Acknowledgement

The authors are deeply indebted to Dr. V. S. Raghunathan, Associate Director, Materials Characterisation Group, Dr. Baldev Raj, Director, Metallurgy and Materials Group, Chemical and Reprocessing Group and Dr. P. Rodriguez, Director, Indira Gandhi Centre for Atomic Research for their keen interest and constant encouragement throughout the course of this work. The authors express their sincere thanks to Prof. K. T. Jacob, Department of Metallurgy, Indian Institute of Science, Bangalore for his useful suggestions.

References

1. H. KLEYKAMP, *J. Nucl. Mater.* **131** (1985) 221.
2. K. SWAMINATHAN, A. M. AZAD, O. M. SREEDHARAN and A. S. DIXIT, *Metals, Mater. Processes* **1** (1989) 207.
3. K. SWAMINATHAN and O. M. SREEDHARAN, *J. Nucl. Mater.* **275** (1999) 225.
4. *Idem.*, *J. Alloys Compds.* **292** (1999) 100.
5. T. B. MASSALSKI, H. OKAMOTO, P. R. SUBRAMANIAN and L. KACPRZAK (eds.), "Binary Alloy Phase Diagrams," 2nd ed. (ASM International, Ohio, 1990).
6. G. I. STRAGUZZI, K. B. BISCHOFF, T. A. KOCH and G. C. A. SCHUTT, *J. Catal.* **103** (1987) 357.
7. V. N. SERGUNKIN, G. K. BORESKOV, V. A. DZISKO, V. P. KARLOV, V. V. KLIMOV, YU. V. PUGACHEV, N. M. SAMOKHVALOVA and D. V. TARASOVA, U.S. Patent, 3,984,353 (October 1976). (Chem. Abst. 86 223365a).
8. E. A. MILITGINA, *USSR Ionnyi Obmen Ionometriya* **4** (1984) 14. (Chem. Abst. 101 221251p).
9. S. HAMPSHIRE and J. COOLICAN, *Mater. Sci. Monograph* **38B** (1987) 1833. (Chem. Abst. 107 145496d).
10. J. N. REIMERS and J. E. GREEDAN, *J. Solid State Chem.* **83** (1989) 20.
11. JCPDS - International Centre for Diffraction Data Version 2.15 PDF-2.
12. E. KOYAMA, I. NAKAI and K. NAGASHIMA, *Nippon Kagaku Kaishi* **6** (1979) 793.
13. E. S. RAMAKRISHNAN, O. M. SREEDHARAN and M. S. CHANDRASEKHARAI AH, *J. Electrochem. Soc.* **122** (1975) 328.
14. C. MALLIKA and O. M. SREEDHARAN, *J. Chem. Thermodyn.* **18** (1986) 727.
15. O. M. SREEDHARAN, M. S. CHANDRASEKHARAI AH and M. D. KARKHANAVALA, *High Temp. Sci.* **9** (1977) 109.
16. O. M. SREEDHARAN, E. ATHIAPPAN, R. PANKAJAVALLI and J. B. GNANAMOORTHY, *J. Less-Common Metals* **68** (1979) 143.
17. R. PANKAJAVALLI, O. M. SREEDHARAN, E. ATHIAPPAN and J. B. GNANAMOORTHY, *J. Electrochem. Soc. India* **30** (1981) 224.
18. H. H. KELLOG, *J. Chem. Engg. Data* **14** (1969) 41.
19. O. M. SREEDHARAN and C. MALLIKA, *Mater. Chem. Phys.* **14** (1986) 375.
20. A. M. AZAD, R. PANKAJAVALLI and O. M. SREEDHARAN, *J. Chem. Thermodyn.* **18** (1986) 255.
21. O. KNACKE, O. KUBASCHEWSKI and K. HESSELMAN (eds.), "Thermochemical Properties of Inorganic Substances," 2nd ed. (Springer-Verlag, Berlin, 1991).
22. R. PANKAJAVALLI and O. M. SREEDHARAN, *J. Mater. Sci.* **22** (1987) 177.

Received 22 September 1999
and accepted 17 February 2000